

An Explorative Study of Visual Servo Control with Insect-Inspired Reichardt-model

Haiyan Wu¹, Tianguang Zhang¹, Alexander Borst²,
Kolja Kühnlenz¹ and Martin Buss¹

¹Institute of Automatic Control Engineering (LSR)
Technische Universität München
D-80290 München, Germany

²Department of Systems and Computational Neurobiology
Max Planck Institute of Neurobiology
Am Klopferspitz 18, D-82152 Martinsried, Germany

Email: {tg.zhang, kolja.kuehnlenz, m.buss}@ieee.org,
haiyan.wu@tum.de, borst@neuro.mpg.de

Abstract—In this paper, an insect-inspired motion detector (Reichardt-model) is applied to visual servo control to ensure the stability of the system with high gain and time delay in its feedback. A Reichardt-based control scheme is compared with a conventional visual servoing approach. As a consequence of the specific velocity dependence of the Reichardt-model, the stability margin of the visual servo control is increased and high overall gains, thus, better performance are achievable. The response of the Reichardt-model in the experiment and the control performance of velocity control approach with the Reichardt-model in the closed loop are investigated. The velocity control model is tested on a 1-DOF linear motor module with different feedback gain and different time delay in the loop. The results of simulation and realtime experiments demonstrate the stabilizing character of the Reichardt-based approach.

I. INTRODUCTION

An important issue in the research field of visual servoing is, how to improve the control performance and to ensure the stability in the presence of time delay. Recent research in neurobiology has revealed a stability effect of Reichardt-detectors despite presence of time-delay, which inspired this work on stable visual servoing.

A fly's vision system, e.g. of the blowfly *Calliphora vicina*, comprises a 2D array of photoreceptors followed by motion detectors which are specialized for the detection of optical flow fields of typical motion behaviors [1]. The Reichardt-detector [2] and its variants [3][4][5] are well-known motion detector models which are applied to simulate the fly's motion detection system. It has been demonstrated in [6] that, despite the presence of time-delay of sensory input, the Reichardt-model in the optomotor system can lead to a stable performance even if it operates with a high gain in its feedback. Further, the Reichardt-model has the advantage of lower computational cost for calculating optical flow compared with conventional methods, e.g. SSD, Horn&Schunck method etc. Therefore, the Reichardt-model has benefits for realtime applications [7][8][9].

For vision-based robot control, there are two traditional

methods: position-based visual servoing (PBVS) and image-based visual servoing IBVS [10]. In addition, new visual servo control techniques have been proposed recently: hybrid visual servo control approaches (e.g. 2 1/2D visual servo control in [11] which uses the error part in 3D Cartesian space and part in 2D image space) and motion-based visual servo control (a nonlinear model is assumed [12] [13]). However, in these papers the stability problem due to time delay of image processing has not been addressed.

In this paper, an elaborated Reichardt-model is introduced and implemented in a velocity control visual servoing scheme. Velocity control models with and without the Reichardt-model are tested in both, simulation and realtime experiments. The models are tested with different feedback gain and different time delay in the closed loop. The realtime experiments are executed on a linear motor module (STB-2510 [14]) with 1-DOF. The control performances of the standard velocity control model and the Reichardt-based model are compared.

The remainder of this paper is organized as follows: firstly, in Section II, the control problem and control law for visual servo control are described. In Section III, the basic Reichardt-model and an elaborated Reichardt-model together with its application in visual servo control are introduced. Simulation results of velocity control are present in Section IV. The experimental setup and experimental results of velocity control with and without the Reichardt-model are shown in Section V and conclusions are given in Section VI.

II. CONTROL PROBLEM OF VISUAL SERVOING

Velocity control with visual servoing is considered in this paper, which is also called motion-based visual servo control. A eye-in-hand structure is selected and the camera is mounted on the end effector. The aim is to control the relative motion \dot{X}_r between the camera and a moving object by moving the robot. A serial n -link rigid robot manipulator

as depicted in Fig. 1 is used and the dynamics of it can be written based on Euler-Lagrangian formulation

$$M(q)\ddot{q} + C(q, \dot{q})\dot{q} + g(q) = \tau, \quad (1)$$

where

q	$n \times 1$	vector of joint displacement;
τ	$n \times 1$	vector of applied joint actuator torques;
$M(q)$	$n \times n$	symmetric positive definite manipulator inertia matrix;
$C(q, \dot{q})\dot{q}$	$n \times 1$	vector of centripetal and Coriolis torques;
$g(q)$	$n \times 1$	vector of gravitational torques.

Through kinematics of the robot, the pose (position and orientation) of the camera frame X_c is expressed with respect to the joint positions. For simplicity, the Cartesian space control is assumed. The block diagram of the velocity control system is given by Fig. 1.

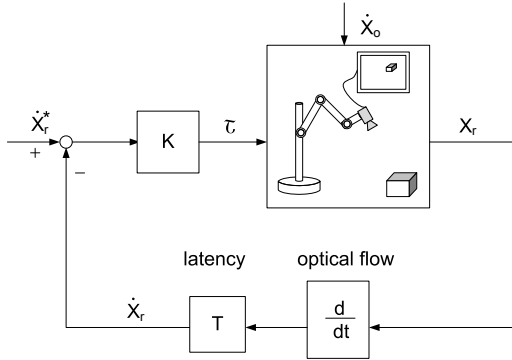


Fig. 1: Block diagram of velocity control visual servoing. Joint torque τ , camera pose X_r , object velocity \dot{X}_o , desired relative motion \dot{X}_r^* .

As shown in Fig. 1, an object moves with the velocity \dot{X}_o in the environment. Therefore, the relative pose of the camera with respect to the moving object is detectable which is denoted by X_r in Fig. 1. The relative motion \dot{X}_r is then obtained through the camera projection, image processing and velocity transformation with latency T . As presented in [15], the velocity of features $\dot{\xi}$ in the image plane can be described in terms of relative camera motion by

$$\dot{\xi} = J(q, \xi, Z)\dot{X}_r, \quad (2)$$

where

$$J(q, \xi, Z) = J_{image}(\xi, Z) \begin{bmatrix} R_c(q) & 0 \\ 0 & R_c(q) \end{bmatrix}, \quad (3)$$

where $J_{image}(\xi, Z)$ is the so-called image Jacobian [15][16][17] and $R_c(q)$ is the orientation of the robot frame with respect to the camera frame. The following control law is used

$$\tau = -K(\dot{X}_r - \dot{X}_r^*), \quad (4)$$

where K is the symmetric positive definite proportional matrix which is chosen by the designer.

It has to be mentioned, that there are different methods of calculating feature velocity (optical flow) from the image sequence, e.g. SSD algorithm, Lucas&Kanade method, Horn&Schnuck method and so on. However, shortcomings exist. By introducing the optical flow calculation into the loop, time-delay due to camera exposure time, time for image transferring and image processing, time for data distribution (a distributed system is selected in the experiment) limits control gains and, thus, performances. When the control gain K increases in presence of latency in the feedback loop, the system given by Fig. 1 will get unstable. To overcome this drawback, a biologically inspired motion detector Reichardt-model is introduced into the system and applied to estimate the optical flow.

III. REICHARDT-MODEL IN IBVS

As demonstrated in [6], when the overall gain of the system is large for the sake of better performance to compensate disturbances efficiently, the optomotor system containing the Reichardt-model in its closed loop does not get unstable, while a standard system without the Reichardt-model becomes unstable. This interesting phenomena inspired us to apply the Reichardt-model to visual servoing. An example of introducing the Reichardt-model into velocity control loop is shown in Fig. 2, where $I(\xi(X_r))$ are the intensity values of the pixels. The Reichardt-model is then applied to each pixel

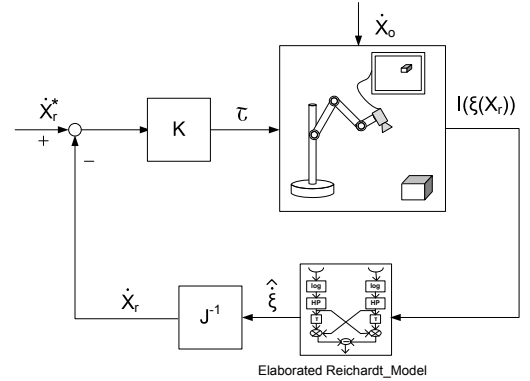


Fig. 2: Block diagram of visual servoing with the Reichardt-model. Intensity values of pixels $I(\xi(X_r))$, estimated optical flow $\hat{\xi}$.

to estimate the corresponding optical flow $\hat{\xi}$. Subsequently, the relative motion of the camera is calculated by

$$\dot{X}_r = J^{-1}(q, \xi, Z)\hat{\xi}. \quad (5)$$

In the following part, the intrinsic properties of the Reichardt-model and an elaborated Reichardt-model are introduced.

A. Reichardt-model

The earliest and probably the most famous model of motion detector inspired by biological systems was developed by Reichardt and Hassenstein in 1956 [2]. Fig. 3 presents a simplified version of the model.

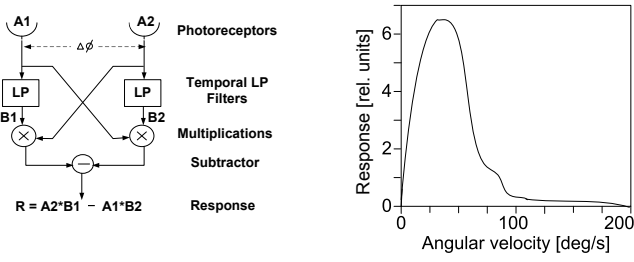


Fig. 3: The simple Reichardt-model [1] ($A1, A2$ are values of pixels, $\Delta\phi$ is the distance between the two input pixels.) and its velocity dependent response.

The motion detector generates a direction sensitive response due to the subtraction between the two symmetric detector halves. The velocity dependence of the response of the Reichardt-model is shown in Fig. 3. The outcome of the Reichardt-model response first increases with increasing velocity, reaches a maximum and then decreases. Hence, the gain of the motion detection system in the fly's optomotor pathway is not constant, but becomes small at high velocities [6].

In order to investigate the response properties of the Reichardt-model in estimating optical flow, two different input signals are tested and the results are shown in Fig. 4 [18]. A positive peak-like signal is generated for the motion to the right and a negative peak-like signal is generated for the motion to the left. The response is zero when no motion exists. However, the response of the Reichardt detector is not always as simple as a peak. For example, as shown in Fig. 4, the sign of the response in f) does not directly indicate motion direction when the input is a step edge. As a result, the simple Reichardt-model could not be directly applied to visual servoing.

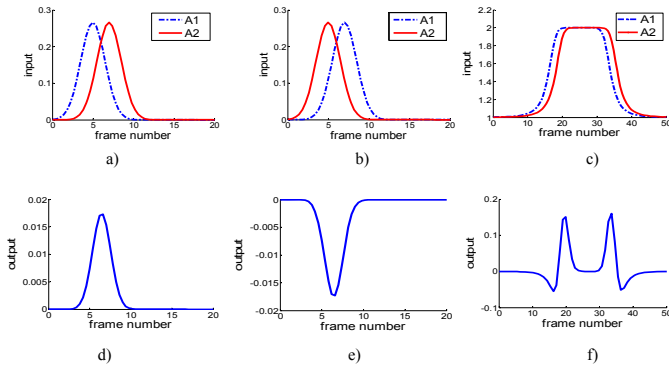


Fig. 4: Response of the Reichardt detector to a moving peak and to a moving pulse [18]. a) a peak moving to right; b) a peak moving to left; c) a pulse moving to right; d) response of a); e) response of b); f) response of c).

B. The Elaborated Reichardt-model

The simple Reichardt detector has two major drawbacks: its response is sensitive to edge contrast, which reduces

robustness to lighting conditions; its response to step edges is complex, which makes scene interpretation difficult. As a result, the simple detector has been improved and two preprocessors are added: logarithmic transformation is applied in order to reduce the sensitivity to lighting conditions directly after the receptors; this is followed by a temporal high-pass filter in order to obtain a simple response to the most common edge type as step edge in natural images.

The elaborated Reichardt-model is shown in Fig. 5, which is proposed in [7]. The moving pulse signal c) in Fig. 4

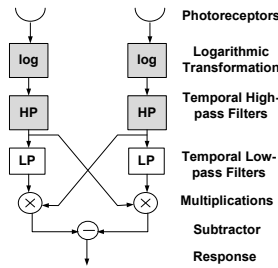


Fig. 5: The elaborated Reichardt-model

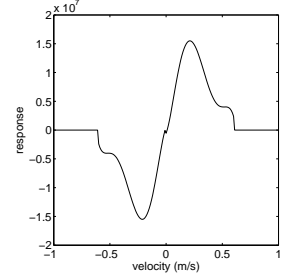


Fig. 6: Response of the Reichardt-model in the experiment.

(or equivalently a moving step edge) is transformed by the temporal high-pass filter into a moving peak (shown in the left of Fig. 7), and thus, leading to a simple response as shown in the right of Fig. 7. Hence, the elaborated Reichardt-

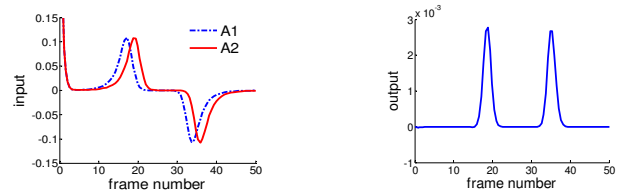


Fig. 7: Response of the elaborated motion detector to a pulse moving to right [18]

model could correctly reflect the direction of the input signal. In image processing, the model is applied to each pixel in both vertical and horizontal directions. The mathematical description of each part of the model (including logarithmic transformation, high-pass filter, low-pass filter) is illustrated in [7].

IV. SIMULATION OF VELOCITY CONTROL

In this part, the standard velocity control model in Fig. 1 and the Reichardt-based velocity control model in Fig. 2 are simulated. In the simulation, a 1-DOF manipulator is modeled. Besides, it is assumed that the target moves with a prior known velocity: $\dot{X}_o = 0.1m/s$. The goal of velocity control is to compensate the motion between the end effector and the target. Thus, the desired relative motion \dot{X}_r^* of the camera with respect to the moving object is zero.

For the standard model, since only 1-DOF manipulator is selected, the relative motion vector of the camera could be

directly obtained from the joint encoder. For the Reichardt-based model, the response of the Reichardt-model with respect to the velocity is firstly observed. In the experiment, the following parameters are chosen for the Reichardt-model: $\tau_H = 3$, $\tau_L = 1.2$, $\phi = 5$. An array of the Reichardt-model is applied to the image and the responses of the Reichardt-model are summed up which represents the optical flow. Based on sampled examples observed in realtime experiments, the response curve given by Fig. 6 is then obtained through interpolation. The response is bell-shaped and is similar to the response of the simple Reichardt-model shown in Fig. 3. Time delay module of 20ms is added in the feedback loop in both models, which simulates the image processing time or transport time. In order to compare the velocity control performance of models with and without the Reichardt-model, the feedback gains in both models that cause end effector motions of 70% of the object velocity are normalized to one (following [6]).

Fig. 8 shows the simulation results of the velocity trajectory of the end effector when the feedback gain is small in both models (*gain* : 1,10). The curves *s_1* and *s_10* are

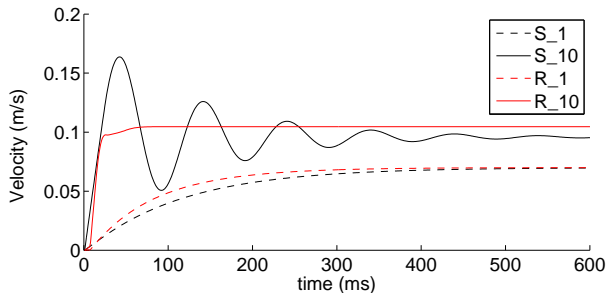


Fig. 8: Velocity trajectory of the end effector when the standard velocity control model or the Reichardt-based model is simulated with small feedback gain: 1,10. (*S_1*, *S_10*: results of standard model; *R_1*, *R_10*: results of the Reichardt-based model.)

velocity trajectories of the standard model when gain is 1 and 10, while *R_1* and *R_10* are velocity trajectories of the Reichardt-based model. In this case, both systems settle down in steady state. However, when the feedback gain increases, the model without the Reichardt-model gets unstable, while model with the Reichardt-model is still in control which oscillates with a certain velocity (shown in Fig. 9).

The results of the simulation show that, when time delay is present and the overall feedback gain increases, the velocity control loop with the Reichardt-model keeps stable due to intrinsic properties of the Reichardt-model, while the standard model becomes unstable.

V. EXPERIMENTS

In this part, the velocity control models simulated in Section IV are tested in realtime experiments. Two experiments are designed and carried out on a linear motor module. The

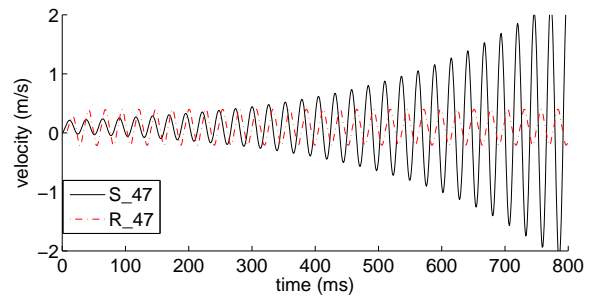


Fig. 9: Velocity trajectory of the end effector when standard velocity control model or the Reichardt-based model is simulated with high feedback gain of 47.

experimental setup and results are described in the following part.

A. Experimental Setup

A linear motor module (STB-2510) depicted in Fig. 10 is selected as the basic module. Since it is a 1-DOF manipula-

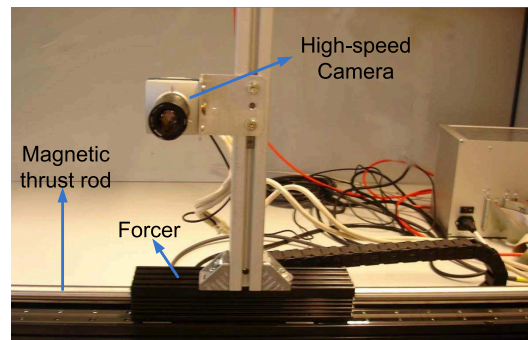


Fig. 10: Experimental Setup

tor, the system is simplified with respect to the simulation. Its end effector is a forcer and moves horizontally. The peak velocity that can be achieved is 4.6m/s. A non-contact position sensor is integrated into the system. Therefore, the velocity of the forcer which is required in the control law (4) can be easily calculated. The system control is implemented using Simulink/Realtime workshop, which runs on a PC (i686, AMD 64 Processor 3000+) with fixed sampling time of 1ms.

A high speed CMOS imaging camera (Mikrotron MC1319) is mounted on the forcer. It provides high speed imaging with up to 500 full frames per second. The intrinsic camera parameters contain: focal length $\lambda = 17mm$, scaling factor $\alpha = 88,888pixels/m$. The captured image is transferred to a host PC (x86_64, AMD 64x2 dual core Processor 5200+) through PCIe.

B. Parameter Settings

Two experiments are carried out. In the first experiment, the standard velocity control model and the Reichardt-based model are tested with different feedback gains (small time delay in the feedback). In the second experiment, different

time delay is added to the feedback loop (small feedback gain). The control performances of these two models with different parameters are presented and compared. The camera works at the framerate of 30fps and has a resolution of 640×480 pixels. The response of the elaborated Reichardt-model in Fig. 6 is applied in the experiments. The velocity of the target \dot{X}_o is set to be $0.1m/s$ and desired relative motion is zero ($\dot{X}_r^* = 0$).

C. Experiment Results 1: different feedback gain

Similar to the simulation in Section IV, the standard model and the Reichardt-based model are tested with different feedback gain. In this experiment, the time delay in the feedback loop of both models is about 20ms. Feedback gains 2, 4, 6, 7 are selected and tested in the experiment.

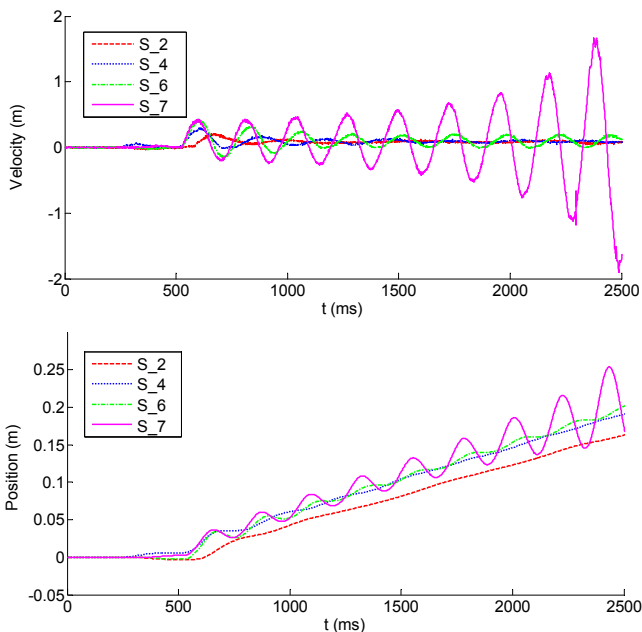


Fig. 11: Velocity and position trajectory of the end effector when the standard model is tested with different feedback gains: 2, 4,6,7. Time delay in the feedback loop is 20ms.

The experimental results are presented in Fig. 11 and Fig. 12 show the velocity and position of the camera with respect to the world frame. As shown in Fig. 11 and Fig. 12, when the feedback gain is small (gain= 2, 4, 6), both models are stable. But for the standard model, when the feedback gain increases, e.g. to 7, the velocity of the end effector gets larger and larger instead of settling down. Thus, the system gets unstable. For the model with the Reichardt-detector in its feedback, the system is still stable when the feedback gain is increased to 7. Only small oscillations are present. It could be concluded from the results of this experiment that the Reichardt-model prevents the system from getting unstable when the overall feedback gain increases and small time delay is present in the feedback loop.

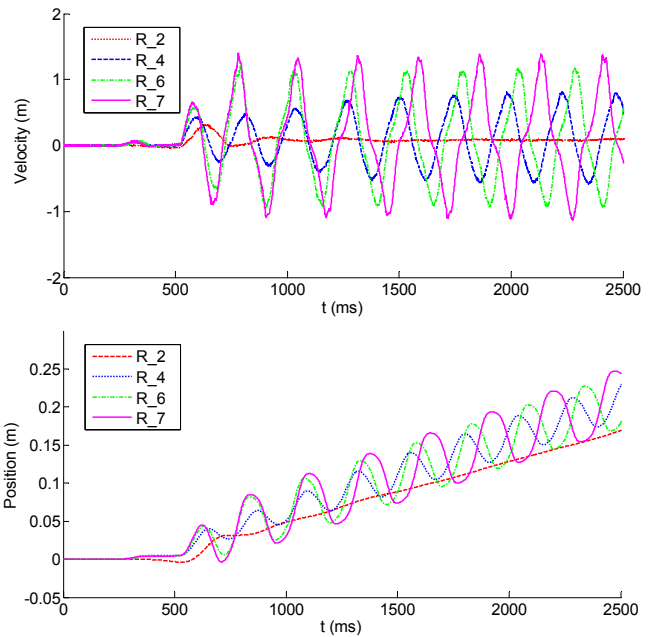


Fig. 12: Velocity and position trajectory of the end effector when the Reichardt-based model is tested with different feedback gains: 2, 4, 6, 7. Time delay in the feedback loop is 20ms.

D. Experiment results 2: different time delay

In this experiment, the feedback gain is set to be constant (gain = 2) and different artificial time delay is added into the feedback loop: 50ms, 100ms, 160ms. The experimental results are presented in Fig. 13 and Fig. 14.

Similar results are observed. When time delay is small (for example: 50ms, 100ms), both models are stable. If the time delay in the feedback is changed to 160ms, for the standard model, the velocity of the end effector increases rapidly and the system tends to become unstable. In contrast, the system is still stable when the Reichardt-model is applied in the closed loop.

It is observed that remaining oscillations are present with the Reichardt-based closed-loop control in both experiments which e.g. could be limit cycles of the quantized and/or non-linear system. This effect is subject to further investigations.

VI. CONCLUSIONS

In this paper, the biologically inspired motion detector Reichardt-model is introduced in visual servo control. As a consequence of the specific velocity dependence of the Reichardt-model, the control system with the Reichardt-model in the feedback loop is demonstrated to have increased stability margin and allow higher overall gains, thus, better performances are achievable. A Reichardt-based control scheme is compared with a conventional visual servo approach. Both approaches are simulated and tested in real-time experiments on a 1-DOF linear motor module. The simulation and experimental results demonstrated the Reichardt-based prevents the system from getting unstable

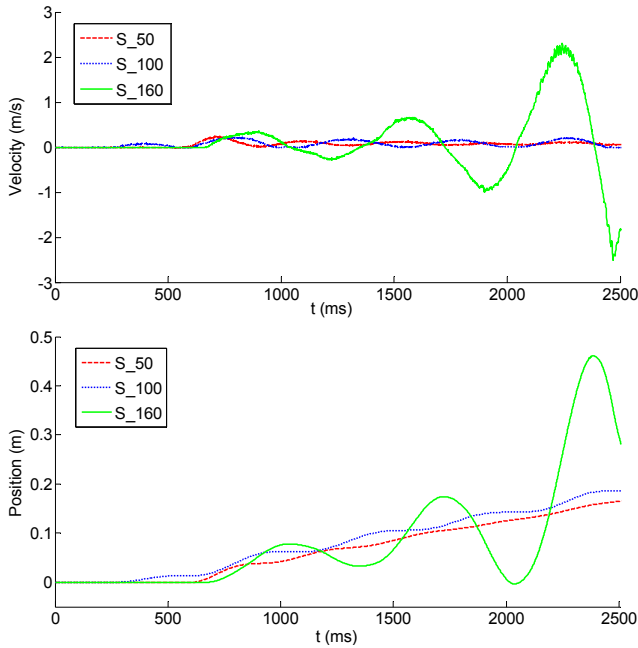


Fig. 13: Velocity and position trajectory of the end effector when the standard model is tested with different time delay in the feedback loop: 50ms, 100ms, 160ms. The applied feedback gain is 2.

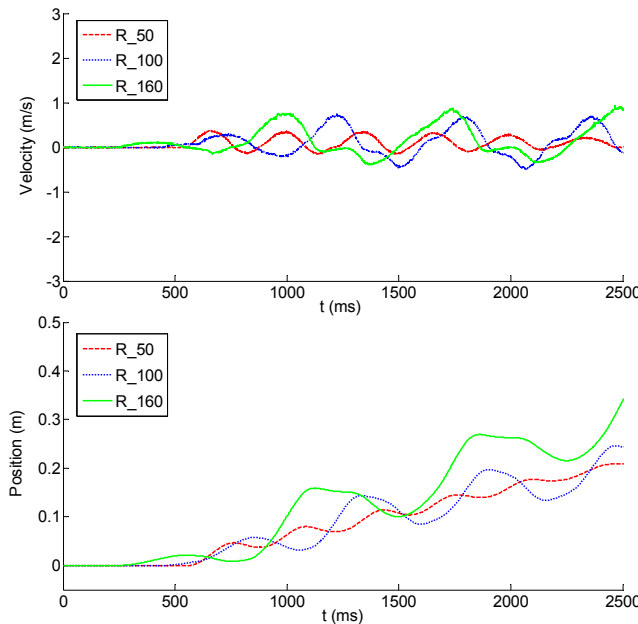


Fig. 14: Velocity and position trajectory of the end effector when the Reichardt-based model is tested with different time delay in the feedback loop: 50ms, 100ms, 160ms. The applied feedback gain is 2.

when feedback gain increases and large time delay is present. In future, the remaining oscillations which are present in the Reichardt-based control scheme (which e.g. could be limit cycles of the quantized and/or nonlinear system) will be further investigated.

VII. ACKNOWLEDGMENTS

This work is supported in part within the DFG excellence initiative research cluster *Cognition for Technical Systems – CoTeSys*, see also www.cotesys.org and the Bernstein Center for Computational Neuroscience Munich, see also www.bccn-munich.de.

REFERENCES

- [1] A. Borst and J. Haag, "Neural networks in the cockpit of the fly," *Journal of Comparative Physiology A*, vol. 188, pp. 419–437, 2002.
- [2] B. Hassenstein and W. Reichardt, "Systemtheoretische Analyse der Zeit-Reihenfolgen, und Vorzeichenbewertung bei der Bewegungsperzeption des Rüsselkaefers," *Naturforsch*, vol. 11b, p. 1956, 1956.
- [3] H. Krapp and R. Hengstenberg, "A fast stimulus procedure to determine local receptive field properties of motion-sensitive visual interneurons," *Vision Research*, vol. 37, pp. 225–234, 1997.
- [4] T. Neumann and H. Bulthoff, "Insect inspired visual control of translatory flight," *Advances in Artificial Life. 6th European Conference, ECAL 2001. Proceedings*, vol. 2159, pp. 627–636, 2001.
- [5] C. M. Higgins and S. A. Shams, "A biologically inspired modular vlsi system for visual measurement of self-motion," *IEEE SENSORS JOURNAL*, vol. 2, pp. 508–528, 2002.
- [6] A. Warzecha and M. Egelhaaf, "Intrinsic properties of biological motion detectors prevent the optomotor control system from getting unstable," *The Royal Society*, vol. 351, pp. 1579–1791, 1996.
- [7] T.G. Zhang, H.Y. Wu, A. Borst, K. Kuehnlencz, and M. Buss, "An fpga implementation of insect-inspired motion detector for high-speed vision systems," *IEEE International Conference on Robotics and Automation (ICRA)*, pp. 335–340, 2008.
- [8] F. and S. Viollet, S. Amic, and N. Franceschini, "Bio-inspired optical flow circuits for the visual guidance of micro-air vehicles," in *Proceeding of the IEEE International Symposium on Circuits And Systems*, 2003.
- [9] E. Nakamura, S. Asami, T. Takahashi, and K. Sawada, "Real time parameter optimization for elementary motion detectors," *IEEE International Conference on Image Processing*, pp. 1065–1068, 2006.
- [10] S. Hutchinson, G.D. Hager, and P. I. Corke, "A tutorial on visual servo control," *IEEE Transactions on Robotics and Automation*, vol. 12, pp. 651–670, 1996.
- [11] E. Malis, F. Chaumette, and S. Boudet, "Positioning a coarse-calibrated camera with respect to an unknown planar object by 2d 1/2 visual servoing," in *Proc. 5th IFAC Symposium on Robot Control*, vol. 2, Nantes, France, 1997, pp. 517–523.
- [12] R. Mahony, P. Corke, and T. Hamel, "Dynamic image-based visual servo control using centroid and optical flow features," *Dynamic Systems, Measurement, and Control*, vol. 130, pp. 1–11, 2008.
- [13] A. Cretual and F. Chaumette, "Positionning a camera parallel to a plane using dynamic visual servoing," *Conf. on Intelligent Robotis and Systems*, vol. 1, pp. 43–48, 1997.
- [14] *Manual of "Models STB2504-2510"*. [Http://www.copleycontrols.com/](http://www.copleycontrols.com/).
- [15] R. Kelly, "Stable visual servoing of camera-in-hand robotic systems," *Transactions on Mechatronics*, vol. 5, pp. 39–48, 2000.
- [16] K. Hashimoto, T. Kimoto, T. i Ebine, and H. Kimura, "Manipulator control with image-based visual servo," *International Conference on Robotic and Automation*, pp. 2267–2272, 1991.
- [17] V. Panwar and N. Sukavanam, "Neural network based controller for visual servoing of robotic hand eye system," *Engineering Letters*, vol. 14, pp. 167–175, 2007.
- [18] F. Faille, A. Borst, and G. Faerber, "Biologically inspired motion detector for video interpretation," *Biological Cybernetics*, 2007, to appear.